

# PROCEEDINGS OF SPIE

[SPIDigitalLibrary.org/conference-proceedings-of-spie](https://SPIDigitalLibrary.org/conference-proceedings-of-spie)

## Fibre Bragg gratings: monitoring of infusion process in liquid composite molding manufacturing

Allsop, Thomas, Tahir, Mohammad, Bhavsar, Kaushal, Zhang, Lin, Webb, David, et al.

Thomas D. Allsop, Mohammad W. Tahir, Kaushal Bhavsar, Lin Zhang, David J. Webb, Jim M. Gilbert, "Fibre Bragg gratings: monitoring of infusion process in liquid composite molding manufacturing," Proc. SPIE 12139, Optical Sensing and Detection VII, 1213913 (17 May 2022); doi: 10.1117/12.2621757

**SPIE.**

Event: SPIE Photonics Europe, 2022, Strasbourg, France

# Fibre Bragg Gratings: Monitoring of infusion process in liquid composite moulding manufacturing

T. Allsop\*<sup>a</sup>, M. W. Tahir<sup>a</sup>, K. Bhavsar<sup>a</sup>, L. Zhang<sup>b</sup>, D. J. Webb<sup>b</sup>, J. M. Gilbert<sup>a</sup>

<sup>a</sup>Dept. of Engineering, Faculty of Science and Engineering, University of Hull, Hull, HU6 7RX, U.K.; <sup>b</sup>Aston Institute of Photonic Technologies (AIPT), Aston University, Aston Triangle, Birmingham B4 7ET, UK

## ABSTRACT

For over three decades, fibre Bragg gratings (FBGs) have been incorporated into buildings and various structures including those made from fibre reinforced polymer (FRP) composites as sensors to monitor the structural health. Furthermore, as FRP composite technology has matured the maximum size of these structures has rapidly increased and thus the manufacturing process itself has become a critical factor in the overall success of these projects both financially from a quality control perspective. An example is ensuring that the infusion of resin into the glass reinforcement mats within the mould has completely wet all the fibre surfaces without leaving dry patches. Checking this issue is problematic as checks can only take place after infusion has completed. We report the use of FBGs to monitor and locate the flow front of a resin-like liquid through glass reinforcement mats within the mould during the infusion process of Resin Transfer Moulding (RTM). During the infusion process, the liquid flow front velocity generates a viscous force that causes the FBGs to produce both a blue and red wavelength shift. We found the wavelength shifts are small but still significant and reasonably repeatable for the same conditions, the same depth, location of sensor within the mould and the same velocity of flow front yielding an error of  $\pm 1.5\text{pm}$ . The blue wavelength shifts ranged from  $8\text{pm}$  to  $17\text{pm}$  depending on the flow front velocity for the “resin-like” liquid. Evidence is presented showing that the main factor of this FBG spectral behaviour is the viscous force.

**Keywords:** Fibre optic sensing, flow front, composite fabrication, fibre Bragg grating, viscous force

## 1. INTRODUCTION

Fibre optic sensors have been incorporated into composite material structures for structural health monitoring (SHM) for over three decades<sup>1</sup>, leading to the creation of many successful and profitable companies<sup>2</sup>. Until now academic and industry researchers have concentrated on the SHM of composite structures during their operation<sup>3</sup>. However, composite structures have become significantly larger<sup>4</sup> and the manufacturing process is now a critical factor in their financial viability due to the defects that may occur in the manufacturing process. A major step in the manufacturing process is the infusion of resin into the glass/carbon reinforcement mats within the mould<sup>4</sup>. The majority of liquid moulding composite processes involve the placing of dry mats within a closed mould then infusing the resin through the dry reinforcement mats. Ensuring that the resin has reached all regions of the mats in the mould is problematic—especially for large and complex moulds. This can also be critical because inspection occurs only after the infusion finishes<sup>5</sup>.

Recently, researchers have reported both blue and red wavelength shifts occurring at the time when the liquid flow front approaches the FBG sensors, thus showing potential for monitoring the flow-front of resin into and through a mould<sup>6-8</sup>, though without offering any in-depth investigation of analysis of the observed spectral behaviour of the FBG sensors

We report here the first in-depth study on the underlying mechanism causing these FBG wavelength shifts and assess their feasibility as a strategy to monitor and to locate the flow front of the resin-type material (the fluid used has a similar viscosity to epoxy resin) during the RTM process of composite manufacturing.. We found the wavelength shifts are small but still significant and reasonably repeatable for the same conditions, with blue wavelength shifts of  $10.3\text{pm} \pm 1.5\text{pm}$ . These conditions are depth, location of sensor within the mould and the same velocity of flow front; between layers 1 and 2, on the mat  $x$ - $y$  plane ( $129\text{mm}$ ,  $122\text{mm}$ , see the reference axis's is shown in Figure 1a ) with a flow front velocity of  $1.69 \times 10^{-3}\text{ms}^{-1} \pm 5 \times 10^{-5}\text{ms}^{-1}$ .

The magnitude of these wavelength shifts depended upon the sensor's location relative to the inlet and outlet vents of the mould. The sensor's blue wavelength shift varied from ~10pm to ~400pm and this spectral behavior occurred at different infusion times, depending upon the location of sensors in the mould and the temporal evolution of the flow-front of the resin..

## 2. EXPERIMENTAL PROCEDURE

To demonstrate the potential of this approach we used a simple mould containing four bidirectional reinforcement glass (BRG) mats. Each BRG mat (22x25cm) consist of ribbons/bundles of glass fibres, typically with diameter of 30 to 60µm and are held together by a waive/stitched thread and are called tows. The BRG mats consist of two layers of tows, with each layer of tows having a different orientation. angles of 45° and 90°, see Figure 1. Furthermore, the stitching holds the BRG mats together and holds the tows in position along with facilitating the handling of the mats. Some initial experiments were conducted to determine the minimum effects of micro bending on the spectra of the FBG sensor when the vacuum is applied; Based on this, the FBG sensors are placed parallel and between adjacent tows at the 90-degree side of the mats, in the x-y plane see Figure 1b. The four BRG mats are symmetrically stacked (z-direction) with the sensor initially placed between BRG mat layer 1 and layer 2 for a series of repeatability experiments, see Figure 1c.

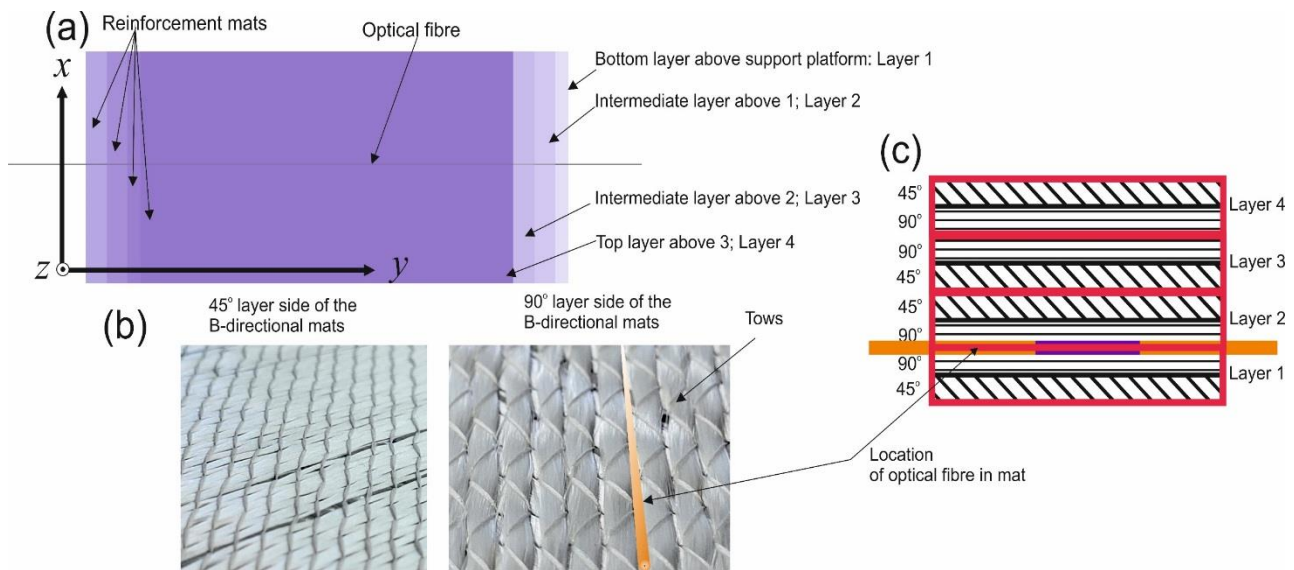


**Figure 1.** The BRG mats and the location and orientation of the FBG sensor within the mats. (a) Schematic top view of the overall layout of the mats and optical fibre with sensor (b) Pictures of either side of the mats. (c) the symmetric arrangement of mats with the four layers stack.

During the repeatability experiments, the orientation of the BRG mats within the mould remained the same, a schematic of the reinforcement orientation is shown in Figure 1c. The liquid used as a resin surrogate was a mixture of glycerol and water (100:17.02 ratio respectively), which has a similar viscosity to the uncured resin. A dye is added to the fluid to ease visual monitoring of the flow front. Epoxy resin was not used due to environmental considerations. Furthermore, the optical fibre that contains the sensor is placed across the entire mould and is anchored/adhered to the sealant that is used to create a vacuum between the vacuum bag and mould support and is referred to as “tacky tape” (ST150 Vacuum bagging Sealant Tape). The experimental arrangement is shown in Figure 2: the mould setup in Figure 2a and optical arrangement in Figure 2b.

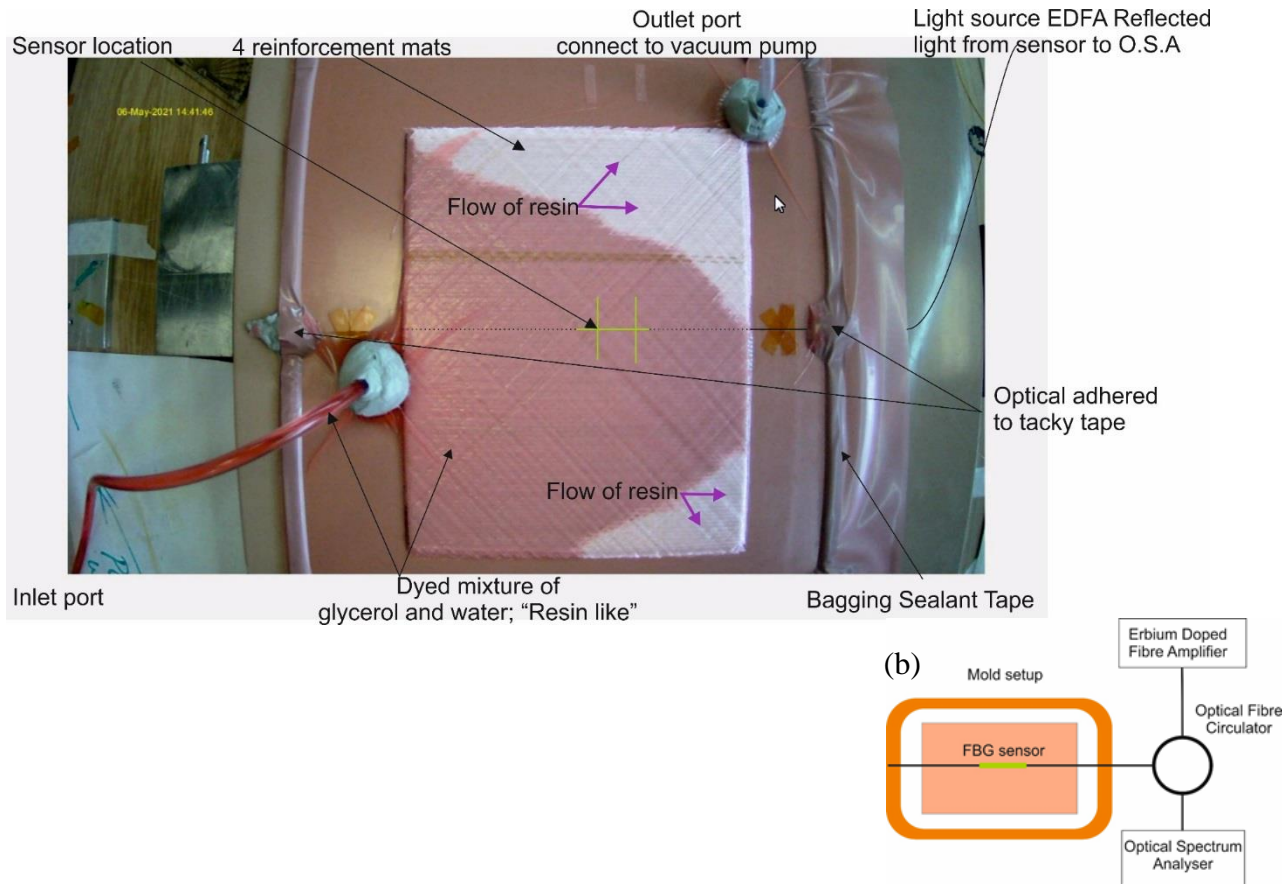


**Figure 2.** The experimental arrangement of apparatus. (a) Picture of the vacuum bag mould (b) Schematic of the optical apparatus.

### 3. RESULTS FROM EXPERIMENTS

#### 3.1 Repeatability experiments

The process is divided into three stages: laying up, application of vacuum and infusion. Initially, the four BRG mats are stack symmetrically on the mould support, shown in Figure 1b with the sensor place in between layers 1 and 2, care is taken to ensure the FBG sensor does not move during the stacking. The tacky is adhered to the mould support and then vacuum plastic film adhered to the tacky tape encapsulating the stack of BRG mats and inlet and out port. Following encapsulation the vacuum rotatory pump is connected outlet port with the inlet closed to create a vacuum. The final stage opening the inlet port valve to allow resin-like liquid to flow into the mould at atmospheric pressure.

During each stage, the FBG sensor undergoes various blue to red wavelength shifts at the various stages of the infusion process. The sensor is located between layers 1 and 2 in the same spatial location within the x-y plane of the BRG mat, an example is shown Figure 2a. The initial red and blue wavelength shifts of the sensor are associated with the manual tensioning of the optical fibre. The initial first wavelength shift during layup is tensioning applied to ensure that the FBG sensor is positioned between tows. The following second wavelength shift is due to the vacuum condition imposed upon the mould itself. These two shifts can vary; the tension red wavelength shift is approximately 100 to 200pm and the second blue wavelength shift is due to the compaction and contraction of the mould due to the vacuum, which yields shifts from 50pm to 200pm. The magnitude of the blue shift depends upon the initial strain given to the fibre during the laying up procedure and vacuum condition created by the rotary vacuum pump, see Figure 3. Following the vacuum stage, the introduction of the resin generates a secondary blue wavelength shift, which then evolves into a red wavelength shift. This occurs as the flow front of resin approaches the FBG sensor and as the sensor is submerged the wavelength shift becomes

red, due to viscous force, experimental evidence will be presented, see Figure 3. The third stage is the continuation of the red wavelength shift as the rest of the mould fills; it is assumed that as the resin fills the mould the compaction gradually reduces and the resin flow exerts an additional strain, see Figure 3.

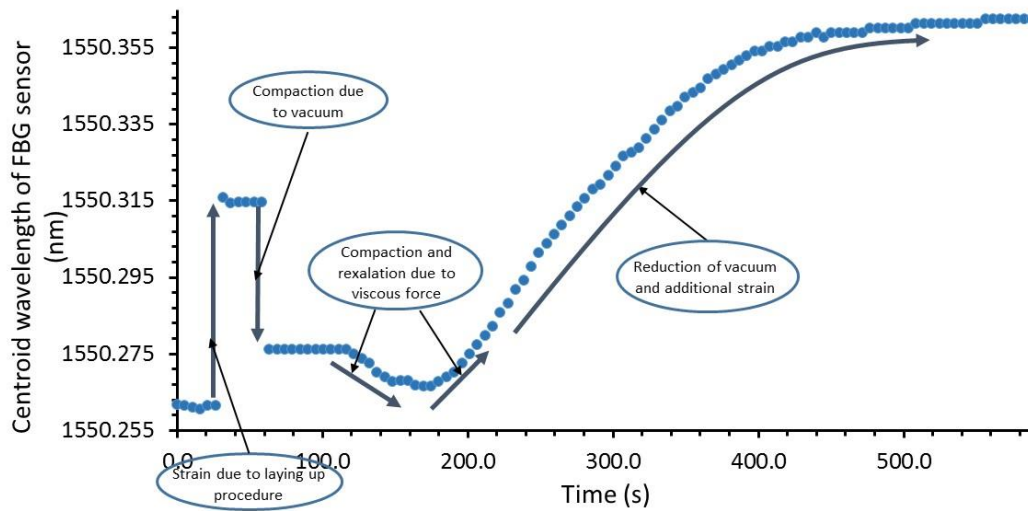


**Figure 3.** Example of the temporal evolution of the spectral behaviour of the FBG sensor during the RTM.

Examples of the wavelength shift measured during the infusion stage are shown Figure 4a. The same spatial location is used for each experiment, and its position is shown in Figure 4b.

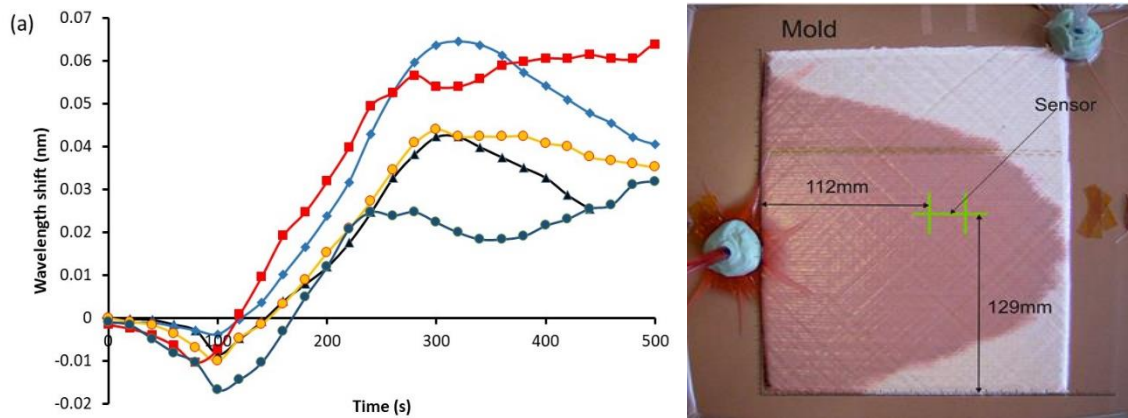


**Figure 4.** (a) Typical spectral response of FBG sensors during the repeatability experiments. (b) The location of sensor.

The repeatability experiments with the sensors involved a uniform FBG of length 25mm, period of 532nm (phase mask  $1.0065\mu\text{m}$ ), at the same location that is shown in figure 4. The spectral behaviour of the FBG sensors was very similar to what other researchers have reported<sup>6-8</sup>. The blue wavelength shifts ranged from 8pm to 17pm depending on the flow front velocity for the “resin-like” liquid. The blue wavelength shift yielded an average an error  $\pm 1.5\text{pm}$ . Example on the wavelength shift and the location of the flow-front along the optical fibre as function of time is shown in Figure 5a. The blue band shows the time that the flow front reaches the sensor. Furthermore, the centroid wavelength<sup>9</sup> of the FBG is shown in the graphs of temporal spectral response of the FBG during infusion, this offers a higher accuracy in the measurement of the wavelength shift<sup>10</sup>.

The significant variation in the blue wavelength shift from the repeatability experiments shown in figure 4a can be explained by looking at the blue wavelength shift as a function of the measured average velocity of the flow front of liquid. The velocity varied from 0.79mm/s to 1.12mm/s. There are several reasons why there are velocity variations, firstly, two

batches of the resin-like liquid were made during the repeatability experiments and there was a small variation in temperature of the laboratory and the effectiveness of the vacuum.

There appears to be a strong relationship between these two parameters, examples of blue wavelength shifts at the same location but differing velocities of the flow front are shown in Figure 5b. Assuming that other conditions are constant in this series of experiments, it is known the viscous force is given by,  $F_v = \mu A \frac{V}{z}$ , where  $\mu$  is viscosity of the fluid and  $A$  is the area of the vacuum mould and  $V/z$  is the rate of shear stress and  $V$  is the velocity profile from the mould support surface upwards and across the mats layers ( $z$ -direction). Furthermore, a Newtonian fluid has a linear relationship between shear stress and velocity gradient across the mats<sup>11</sup>;  $\frac{\partial V}{\partial z}$ , therefore assuming the same velocity profile, the magnitude of the velocity will be proportional to the viscous force, which is seen in Figure 5b. A camera is positioned above the mould, its view can be seen from Figures 2a and 4a. The infusion process is filmed and the flow front is measured from stills from the film at equal time periods to estimate the velocity.

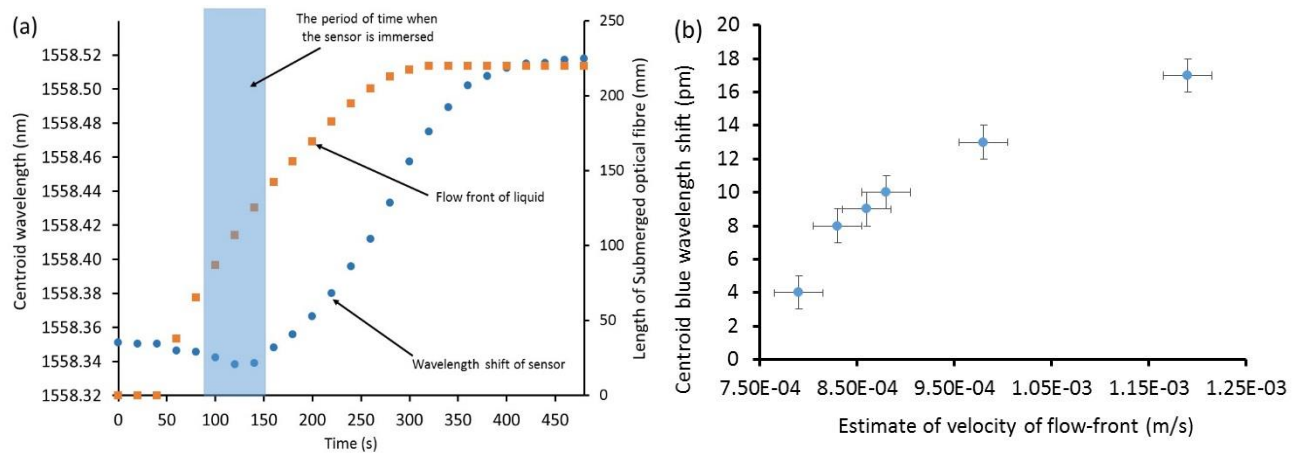


**Figure 5.** Typical results from the repeatability experiments the sensor is between layers 1 and 2, on the mat  $x$ - $y$  plane (129mm, 122mm) (a) Firstly, the centroid wavelength shift of the FBG sensor during the infusion of the mould as a function of time during the infusion of the liquid, secondly the position of the flow front of the liquid along the length of the optical fibre containing the sensor during the infusion of the mould. (b) The measured blue wavelength shift of the FBG sensor as a function of the measured flow-front velocities measured from the camera data.

### 3.2 Viscosity experiments

Following the experimental observations of the spectral behaviour of the sensors made in the initial sets of experiments, a series of infusion experiments were conducted with liquids with different viscosities. The viscosity was adjusted by varying the ratio of water to glycerol was varied from 17.02/100 to pure glycerol, resulting in the calculated viscosity values are shown in Table 1. The sensor was placed at the same spatial location in the  $x$ - $y$  plane and between the 1<sup>st</sup> and 2<sup>nd</sup> layers and parallel to the tows and laid on the 90° side of the BRG mat within the mould. The overall spectral response to the various viscosities is shown in Figure 6. There are several observations: firstly, the response occurs more rapidly for the lower viscosity fluid since it fills into the mould more quickly. Secondly, that as the viscosity increases the blue shift increases, see Figure 7a, which is a direct indicator that the overall force on the sensor is increasing. This is expected since the viscosity of the liquid is directly proportional to the viscous force generated by the ingress of the liquid during infusion. Thirdly, the velocity of the flow-front decreases as the viscosity increases, see Figure 7b, which indicates that the magnitude of velocity is not the dominating factor. The friction of the liquid (viscosity) to the supporting surface and the layers within the mould is higher, and thus the rate of velocity change of the liquid away from the support surface through the mats in the direction would be greater. Therefore, so is the rate of shear stress from the supporting surface and across the mat layers, thus the a dominant factor is the viscous force. This assertion is further strengthened by the results given in the Figure 5a; for a liquid with the same viscosity as the velocity increases, the force will increase.

Table 1. The overall characteristics of the viscosity experiments

Water volume ratio	Glycerol volume ratio	Calculated viscosity (Nsm <sup>-2</sup> )	Velocity of liquid in the mould at the sensor location (ms <sup>-1</sup> )	Maximum blue wavelength shift (pm)
17.02	100	0.12	0.001655	4.8
12	100	0.19005	0.001143	9
8	100	0.2936	0.0008171	11.56
4	100	0.49027	0.0006148	16.56
2	100	0.65682	0.0004306	21.8
0	100	0.90568	0.0002661	24.56

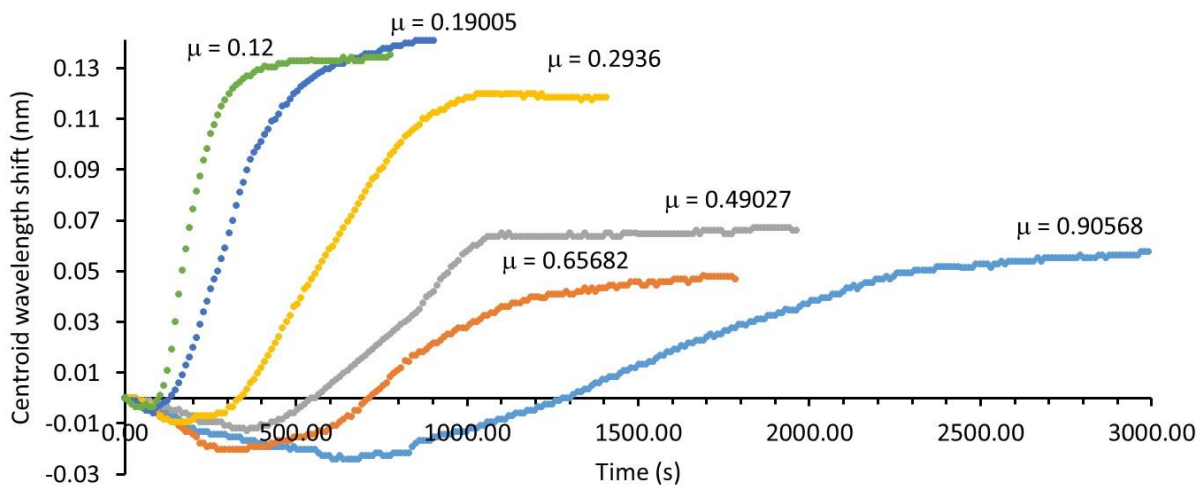


Figure 6. The spectral evolution of the central wavelength of the FBG sensor during the infusion process with the sensor at the same location with different liquid viscosities.

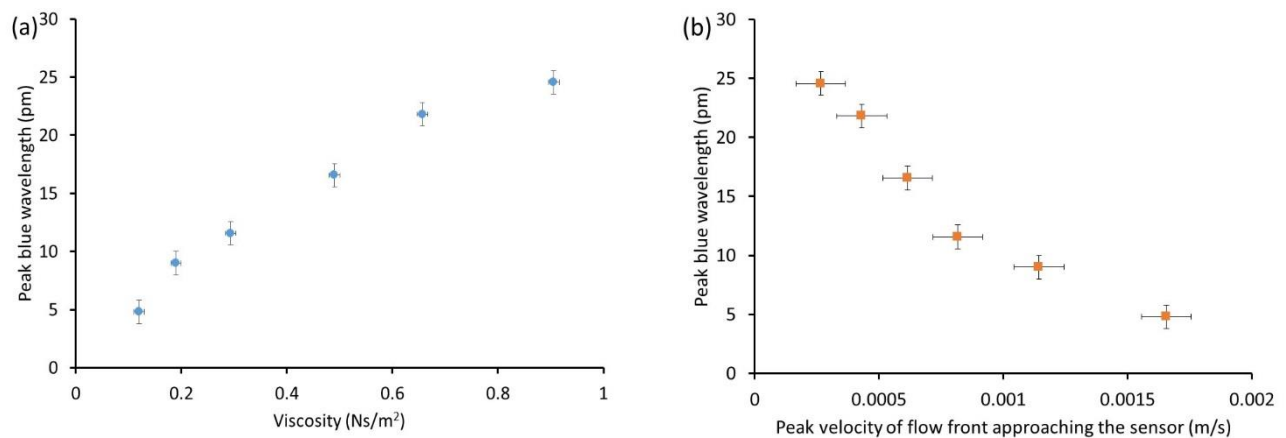


Figure 7. The spectral wavelength response of the FBG sensor during the infusion process as a function of (a) viscosity of the liquid (b) the peak velocity of the liquid approaching the sensor.

## 4. CONCLUSION

A series of experiments were conducted to investigate the possibilities of using FBGs to monitor the flow front of resin during the infusion process of the manufacturing of composite structures. It was found that FBGs experienced a blue and red wavelength shift, with typical blue wavelength shifts of 10pm and for a given set of conditions that this spectral effect is repeatable. Furthermore, evidence has been presented to illustrate that this spectral effect is due to the viscous force created by the flow front of the ingression of liquid. This importantly shows that the FBG sensor spectral behaviour can be understood in terms of the physical conditions that are occurring within a mould during the RTM process, the flow front of the resin during infusion. Therefore, were there is a flow front of resin into a mould this effect and FBG have the the potential to be used to monitor this critical stage in the manufacturing of fibre reinforced polymer composites.

## 5. ACKNOWLEDGEMENTS

The work was funded by the UK Engineering and Physical Sciences Research Council; EPSRC Prosperity Partnership 'A New Partnership in Offshore Wind' EP/R004900/1 and EPSRC Supergen ORE Hub, EP/S000747/1.

## REFERENCES

- [1] W. L. Schulz, L., E. Udd, J. M. Seim, G. E. McGill, "Advanced fiber-grating strain sensor systems for bridges, structures, and highways." In *Smart Structures and Materials 1998: Smart Systems for Bridges, Structures, and Highways*, vol. 3325, pp. 212-221. International Society for Optics and Photonics, 1998.
- [2] B. Culshaw, Brian, A. Kersey, "Fiber-optic sensing: A historical perspective." *Journal of lightwave technology* 26, no. 9, 1064-1078, 2008.
- [3] F. Lambinet, Z. S. Khodaei, "Measurement platform for structural health monitoring application of large scale structures." *Measurement*, 110675, 2022.
- [4] Q. Govignon, S. Bickerton, J. Morris, P.A. Kelly, "Full field monitoring of the resin flow and laminate properties during the resin infusion process", *Composites Part A: Applied Science and Manufacturing*, 39 (9), 1412-1426, 2008.
- [5] K. Potter, B. Khan, M. Wisnom, T. Bell, and J. Stevens, "Variability, fibre waviness and misalignment in the determination of the properties of composite materials and structures.", *Composites Part A: Applied Science and Manufacturing* 39, no. 9, 1343-1354, 2008.
- [6] M. Nielsen, J. W. Schmidt, J. H. Høgh, J. P. Waldbjørn, J. H. Hattel, T. L. Andersen, and C.M. Markussen, "Life cycle strain monitoring in glass fibre reinforced polymer laminates using embedded fibre Bragg grating sensors from manufacturing to failure.", *Journal of Composite Materials* 48, no. 3, 365-381, 2014.
- [7] M. Nielsen, J. W. Schmidt, J. H. Hattel, T. L. Andersen, and C. M. Markussen. "In situ measurement using fbgs of process- induced strains during curing of thick glass/epoxy laminate plate: experimental results and numerical modelling.", *Wind energy* 16, no. 8, 1241-1257, 2013.
- [8] J-M. Jeong, S. Eum, S. Y. On, K. Kageyama, H. Murayama, K. Uzawa, and S. S. Kim. "In-situ resin flow monitoring in VaRTM process by using optical frequency domain reflectometry and long-gauge FBG sensors.", *Composite Structures*, 115034, 2021.
- [9] Bronstein AM, Kimmel R. *Numerical Geometry of Non-rigid Shapes*. Berlin: Springer Science & Business Media; 2008.
- [10] P.S. Shiakolas, D. Koladiya, J. Kebrle. "On the optimum synthesis of six-bar linkages using differential evolution and the geometric centroid of precision positions technique." *Mechanism and Machine Theory* 40, no. 3, 319-335, 2005.
- [11] Massey, B.; Ward-Smith, J. *Mechanics of Fluids* (8th ed.), Taylor & Francis, 2005.